Journal of Cerebral Blood Flow & Metabolism (2015) 35, 818–827

www.jcbfm.com

OPEN

ORIGINAL ARTICLE

Brain barrier properties and cerebral blood flow in neonatal mice exposed to cerebral hypoxia-ischemia

C Joakim Ek[1], Barbara D'Angelo[1], Ana A Baburamani[1,2], Christine Lehner[3], Anna-Lena Leverin[1], Peter LP Smith[1], Holger Nilsson[1], Pernilla Svedin[1], Henrik Hagberg[2,4,5] and Carina Mallard[1,5]

Insults to the developing brain often result in irreparable damage resulting in long-term deficits in motor and cognitive functions. The only treatment today for hypoxic-ischemic encephalopathy (HIE) in newborns is hypothermia, which has limited clinical benefit. We have studied changes to the blood–brain barriers (BBB) as well as regional cerebral blood flow (rCBF) in a neonatal model of HIE to further understand the underlying pathologic mechanisms. Nine-day old mice pups, brain roughly equivalent to the near-term human fetus, were subjected to hypoxia-ischemia. Hypoxia-ischemia increased BBB permeability to small and large molecules within hours after the insult, which normalized in the following days. The opening of the BBB was associated with changes to BBB protein expression whereas gene transcript levels were increased showing direct molecular damage to the BBB but also suggesting compensatory mechanisms. Brain pathology was closely related to reductions in rCBF during the hypoxia as well as the areas with compromised BBB showing that these are intimately linked. The transient opening of the BBB after the insult is likely to contribute to the pathology but at the same time provides an opportunity for therapeutics to better reach the infarcted areas in the brain.

Journal of Cerebral Blood Flow & Metabolism (2015) **35,** 818–827; doi:10.1038/jcbfm.2014.255; published online 28 January 2015

Keywords: blood–brain barrier; brain injury; cerebral blood flow; hypoxia-ischemia; neonate; tight- junction

INTRODUCTION

Hypoxic-ischemic (HI) insults to the developing brain can cause unrepairable brain damage resulting in long-term neurologic deficits such as cerebral palsy. The exact mechanisms behind these pathologies are still unclear and there are only limited therapies to improve the outcome of hypoxic-ischemic encephalopathy (HIE).[1] Both the developing and adult brain is normally protected by a series of barrier mechanisms that come under the term blood–brain barrier (BBB).[2] These mechanisms are situated at the level of cerebral blood vessels, the BBB, and the choroid plexus, the blood–cerebrospinal fluid (CSF) barrier (BCB), and encompass both outward and inward transport systems as well as highly restrictive tight junctions that form the physical barrier at the interfaces between blood, CSF, and brain. These barrier mechanisms are formed early in development and are important for establishing a stable favorable environment and facilitating nutritional support for all the different cells in the brain during brain maturation.[2] Thus, disturbances to these barrier mechanisms could result in changes to developmental processes. There is a large body of work on disturbances to barrier function after hypoxia to the adult animal but very few focused on the developing brain.[3,4] However, most of these studies do indicate that barrier function is disturbed during HI insults in the neonate.[3] We undertook the present study to better define changes to the BBB and BCB as well as to understand the underlying mechanisms behind barrier disturbances after neonatal HI. In addition, regional cerebral blood flow (rCBF) measurements were conducted after the insult since this is important, not only in relation to BBB permeability experiments but also for understanding the neuropathology, with no previous rCBF measurements undertaken in neonatal mice during or after HI. Understanding the permeability changes to the BBB after HI insult is also pivotal since the barrier normally excludes many potentially therapeutic compounds from entering the brain. An episode of HI was induced in 9-day-old mice, brain equivalent to the near-term human fetus, and the BBB permeability and CBF were measured at different time points after the insult. Our results show that there is a transient opening of the barrier, which appears to resolve with time. This is associated a reduction in tight-junctional protein levels as well as protein distribution after HI. However, gene expression of tight-junctional proteins is upregulated indicating compensating mechanisms at the brain barrier forming cells. Changes in rCBF showed a tight correlation with brain regions of damage as well as barrier

[1]Department of Physiology, Institute for Neuroscience and Physiology, Sahlgrenska Academy, University of Gothenburg, Gothenburg, Sweden; [2]Centre for the Developing Brain, Division of Imaging Sciences and Biomedical Engineering, King's College London, King's Health Partners, St. Thomas' Hospital, London, UK; [3]Spinal Cord Injury and Tissue Regeneration Center Salzburg, Department of Traumatology and Sport Injuries, Institute of Tendon and Bone Regeneration, Paracelsus Medical University, Salzburg, Austria; Austrian Cluster for Tissue Regeneration and [4]Departments of Obstetrics and Gynecology, Institute for Clinical Sciences, Sahlgrenska Academy, University of Gothenburg, Gothenburg, Sweden. Correspondence: Dr CJ Ek, Departments of Neuroscience and Physiology, Sahlgrenska Academy, University of Gothenburg, Gothenburg, Sweden.
E-mail: joakim.ek@neuro.gu.se
[5]Shared senior authorship.
This research received financial assistance from the Swedish Medical Research Council (VR 2009-2630, VR 2012-2992, VR 2012-3500), a government grant to a researcher in Public Health Service at the Sahlgrenska University Hospital (ALFGBG-142881, ALFGBG-426401), European Union grant FP7 (Neurobid, HEALTH-F2-2009-241778), the Leducq Foundation (DSRR_P34404), the Wellcome Trust (WT094823MA), Åhlén-stiftelsen, Olle Engkvist Foundation, Wilhelm and Martina Lundgren Foundation, Magnus Bergwall Foundation and the Åke Wiberg Foundation.
Received 13 August 2014; revised 5 December 2014; accepted 8 December 2014; published online 28 January 2015

opening, with some minor differences compared with previous rCBF measurements in neonatal rats.[5–8]

MATERIALS AND METHODS

Neonatal Hypoxic-Ischemic Injury

All experiments were conducted in accordance with Department of Agriculture (Sweden) ethics regarding animal experimentation and with the approval of the Gothenburg animal ethics committee. Experimentation was performed on C57/Bl6 mice that were housed at the Laboratory for Experimental Biomedicine, University of Gothenburg, on a 12-hour light/dark cycle with free access to food and water. A unilateral HI brain injury was induced at postnatal day 9 (P9) in mice as described in detail previously.[9] Day of birth was assigned as P0. Briefly, the left carotid artery was permanently ligated under isoflurane anesthesia and skin closed using surgical glue with surgery typically lasting 3 to 5 minutes. The pups were returned to the mother for 1 hour and then introduced to a 10% oxygen concentration chamber (air/nitrogen gas mixture; 36 °C) for 50 minutes. No animals died as a result of HI. Pups were then returned to the mother and collected at different time intervals after HI for BBB permeability experiments, rCBF, protein analysis (immunocytochemistry/western blotting), or gene expression. Analysis was performed by persons blinded to group belonging.

Brain Barrier Permeability

Sucrose permeability. Assessments of BBB and BCB sucrose permeability were performed at 2 hours ($n=6$), 6 hours ($n=14$), 24 hours ($n=13$), 3 days ($n=6$), or 7 days ($n=7$) after HI along with P9 naïve animals ($n=14$). Each group contained animals from 3 to 5 litters. Animals were injected with ^{14}C-sucrose (342 Da) intraperitoneally (0.2 μCi/g body weight; 10 μL injection/g animal) and killed at 30 minutes by pentobarbital injection. Animals also a received an intraperitoneal injection of ^{3}H-inulin (~5,000Da; 5 μCi/animal; 20 μL injection) at 3 minutes before killing to estimate vascular space in brain tissues. Blood was collected from the heart and spun to separate plasma. Cerebrospinal fluid was collected from the cisterna magna by a small glass capillary (blood contaminated samples discarded),[10] brain dissected out and further separated into different regions: left/right hippocampus, cortex, striatum/thalamus, cerebellum, and brainstem. Brain tissue samples were dissolved using soluene-350. Isotope activity in each fluid or tissue sample was determined by liquid scintillation counting (LSC) with window settings for simultaneous determination of ^{14}C/^{3}H and calculated as activity/mg sample. Since inulin was administered only 3 minutes before killing the animals and is a much larger marker than sucrose it can be assumed that it is only distributed within the vasculature of the brain, thus, the brain/plasma ^{3}H-inulin activity ratios were used as a measure of residual blood volume. This volume was then used to determine the ^{14}C activity of the trapped blood in individual brain tissues, which in turn was subtracted from all ^{14}C tissue activities to yield the true ^{14}C activity in brain tissues parenchyma. Brain/plasma or CSF/plasma sucrose concentration ratios were used as a measure of blood–brain or blood–CSF permeability as previously described.[10]

Albumin immunoreactivity. Blood–brain barrier permeability to endogenous albumin (~66,000Da) was determined immunohistochemically at 2, 6, 24 hours and 3 days after HI along with P9 naïve controls. This abundant plasma protein is unlikely to be synthesized within the brain making it a suitable endogenous larger-sized permeability marker. Paraffin sections of the brain at the level of the hippocampus were deparaffinized and blocked as below and incubated with goat anti-albumin (1:6,000; Abcam, Cambridge, UK, Cat# ab19194) overnight followed by biotinylated horse anti-goat (1:250; Vector, Peterborough, UK) and further processed as below.

Immmunohistochemistry

After HI, animals were killed by an intraperitoneal injection of pentobarbital at 2, 6, and 24 hours for immunohistochemical analysis along with P9 naïve controls ($n=5$ for each group; 2 to 3 mixed litters). Pups were transcardially perfused with heparinized saline followed by cold Histofix (Histolab, Gothenburg, Sweden) with flow rate set to the estimated total blood volume (10% of body weight) per minute to minimize the risk of damaging cerebral vessels. Brains were dissected out and postfixed overnight in fridge before embedded in paraffin. Coronal 7 μm sections were cut of brains and sections at two different hippocampal levels were selected for immunohistochemistry. After deparaffination, rehydration and antigen retrieval by boiling in citrate buffer (pH 6) or protease digestion (*Streptomyces griseus*, Sigma, St. Louis, MO, USA; 1 mg/mL at 37°C) for 10 minutes, sections were treated with 3% H_2O_2 and incubated with the following primary antibodies overnight: mouse anti-MAP-2 (1:2,000; clone HM-3, Sigma), mouse anti-claudin-5 (1:1,000; Invitrogen, Camarillo, CA, USA), rabbit anti-occludin (1:100; Invitrogen, Cat#71-1500), anti ZO-1 (1:100, Invitrogen Cat#61-7300), rabbit anti-active caspase-3 (1:100; BD Pharmingen, Stockholm, Sweden, Cat#559565). Sections were then incubated with biotinylated secondary antibodies (2 hours), followed by avidin-peroxide complex (1 hour; ABC kit PK-6100, Vector), or HRP-conjugated antibodies against the appropriate species (1:250; Vector). All sections were developed with DAB kit (SK-4100, Vector) according to manufacturer's recommendations with or without nickel enhancement.

Further analysis of claudin-5 expression was performed at 6 hours after HI since this protein has been directly shown to affect barrier permeability in neonates.[11] Brains were collected at 6 hours after HI ($n=3$), fixed as above and cryoprotected in 30% sucrose before 30 μm frozen sections were cut with a Leica freezing microtome. Sections were blocked in 4% horse serum before incubation with mouse anti claudin-5 antibodies (1:1,000) and goat anti-albumin antibodies (1:6,000). Sections were then incubated with Alexafluor-488/594 conjugated antibodies against appropriate species (1:1,000; Vector) before examination under a Leica TCS SP2 confocal microscope (Leica, Bromma, Sweden). For all immunoreactivity, control sections omitting primary antibodies resulted in no detectable signal.

Analysis of tissue sections. Quantitative measurements of the MAP-2 and albumin immunoreactivity area were performed whereas all other immunoreactivity was assessed qualitatively. For measurements, two pairs of adjacent sections (100 μm apart), with each pair stained for the two markers, at hippocampal levels were photographed and the MAP-2-negative area (indicating loss of gray matter) or albumin-positive area in the left hemisphere was outlined and measured using imageJ (1.64a; NIH, Bethesda, MD, USA) freeware. The average MAP2^{-} and albumin^{+} area was calculated for each brain.

Caspase-3 Activity, Quantitative PCR, and Western Blotting

Groups of pups were killed by an overdose of pentobarbital at 6 hours after HI ($n=10$) and the right/left hippocampus, cortex, and telencephalic choroid plexuses dissected out and samples used for caspase-3 activity assay (brain samples only), real-time PCR to quantify gene expression, and western blotting to quantify protein expression (brain samples only).

Caspase-3 activity assays. To investigate cell death mechanisms after HI, a fluorometric assay of Caspase-3 activity was performed as previously described.[12] Peptide substrate, Ac-Asp-Glu-Val-Asp-aminomethyl coumarine (Ac-DEVD-AMC; #SAP3171v, Peptide Int., Louiseville, KY, USA) was mixed with samples of hippocampus and cortex. Cleavage of the substrate was measured at 37°C using a Spectramax Gemini microplate fluorometer (Molecular Devices, Sunnyvale, CA, USA), with an excitation/emission wavelength of 380/460 nm. The degradation was followed at 2-minute intervals and *V*-max was calculated from the entire linear part of the curve. Standard curves with AMC (7-amino-4-methyl-coumarin) were used to express the data in picomoles of AMC formed per minute and per milligram of protein.

Western blotting. For immunoblotting analysis, brains were homogenized by sonication in ice-cold PBS containing 5 mmol/L EDTA, protease and phosphatase inhibitor cocktails (Sigma-Aldrich, Saint Louis, MO, USA). The protein concentration was determined using a Nanodrop 2000 (Thermo Scientific, Waltham, MA, USA). Sample lysates were mixed with 4X LDS Sample Buffer (NuPage, Invitrogen) and heated (70°C) for 10 minutes. Total proteins (15 μg/well) were resolved on 4% to 12% Tris-Bis gels (NuPage) or on 3% to 8% Tris-Acetate-gels (ZO-1 only) and transferred onto reinforced nitrocellulose membranes (Schleicher & Schuell, Dassel, Germany). Membranes were blocked in 30 mmol/L Tris–HCl (pH 7.5), 100 mmol/L NaCl and 0.1% Tween-20 (TBS-T) containing 5% fat-free milk powder for 1 hour and then incubated with the following primary antibodies overnight: mouse-anti claudin-5 (1:500), rabbit anti-occludin (1:200), rabbit anti-ZO-1 (1:500), and rabbit anti-β-actin (1:10,000; Sigma-Aldrich). After washing, the membranes were incubated with the appropriate peroxidase-labeled secondary antibody (Vector Laboratories, Burlingame, CA, USA) for 1 hour and visualized using a Super Signal Western Dura substrate (Pierce, Rockford, IL, USA) and a LAS 1000-cooled CCD camera (Fujifilm, Tokyo,

Japan). Immunoreactive bands were quantified using the Image Gauge software (Fujifilm) with β-actin used as a loading control.

Quantitative PCR. Brain RNA was extracted with the RNeasy Lipid Tissue Mini Kit (Qiagen, Solna, Sweden) and choroid plexus RNA extracted with the RNeasy Micro Kit (Qiagen). Total RNA was measured in the Nanodrop 2000 (Thermo Scientific) at 260 nm absorbance. First-strand cDNA was synthesized from 1 μg RNA from brain or 200 ng RNA from choroid plexus, using the QuantiTect Reverse Transcription Kit (Qiagen). Each PCR amplification containing diluted cDNA, Quanti Fast SYBR Green PCR Master Mix (Qiagen), and PCR primer were run on a LightCycler 480 (Roche, Bromma, Sweden). The following primers were used: Cldn5 (QT00254905), Ocln (QT00111055), (ZO-1) Tip-1 (QT00493899), Cldn1 (QT00159278), Gapdh (QT01658692), and Rn 18 S (QT01036875), all from Qiagen. The amplified transcripts were quantified with the relative standard curve and normalized against the reference genes Rn 18 S and glyceraldehyde 3-phosphate dehydrogenase.

Measurements of Cerebral Blood Flow

Regional cerebral blood flow was measured by the iodoantipyrine method [6,7,13–15] before (1 hour after ligation), during (20 to 30 minutes and 50 to 60 minutes), and after hypoxia (2 hours, 6 hours, and 24 hours) as well as in P9/10 days old naïve control mouse pups. Measurements were made in the whole hemispheres by ^{14}C LSC ($n = 5$ to 15 animals/group) or in different brain regions (cortex, hippocampus, striatum, white matter, and thalamus; $n = 5$ animals/group) from autoradiograms. Five μCi (50 μL) 4-Iodo[N-methyl-^{14}C]antipyrine (American Radiolabeled Chemicals, Saint Louis, MO, USA) in saline was injected subcutaneously. After 60 seconds the mouse was decapitated and 10 μL blood was collected in Soluene-350 (Perkin-Elmer, Waltham, MA, USA) and the left/right hemispheres were separated in tubes containing Soluene-350, Perkin-Elmer. After samples were dissolved, 4.5 mL Ultima Gold (Perkin-Elmer) added and the radioactivity in samples measured by LSC (Packard Instrument, Meridan, CT, USA). Brains for autoradioagraphy were frozen in 2-methylbutane on dry ice. Coronal frozen sections, 20 μm, were cut and mounted on Plus glasses, dried and exposed on Carestream Kodak BioMax MS film (Sigma) together with [^{14}C]methacrylate standards (American Radiolabeled Chemicals). Regions and standards were analyzed in a CCD Camera (FujiFilm) and with Multi Gauge software (FujiFilm). For each region, the average blood flow was calculated from autoradiograms of 2 to 4 sections depending on brain region.

Statistics

Data were analyzed using one-way analysis of variance (ANOVA) with individual differences determined with Fisher's least significant difference (LSD) or by two-tailed *t*-test as appropriate (indicated in figure legends) using SPSS software, IBM, Armonk, NY, USA ($\alpha = 0.05$). Data are presented as mean ± s.e.m. unless otherwise stated.

RESULTS

Blood–Brain Barrier Permeability

We used sucrose CSF/plasma and brain/plasma ratios to assess blood–CSF and BBB permeability after HI with ratios corrected for residual blood space. Initially, brain/plasma sucrose concentration ratios for the right (nonligated) hemisphere were compared with littermate controls (naïve animals). As seen in Supplemetary Figure 1, these ratios were almost identical showing that BBB permeability is not altered in the right hemisphere after HI. The right hemisphere was therefore used as an internal control and concentration ratios were calculated between the left (ligated)/right hemispheres. The CSF/plasma concentration ratios were compared with ratios from littermate controls (naïve pups). In Figure 1, these ratios are presented for the hippocampus, cortex, striatum/thalamus, and also the CSF/plasma ratios. Significantly higher permeability ratios were found at 2 hours after HI only in hippocampus ($P = 0.047$). At 6 hours, the highest ratios were found across all time points in the hippocampus, cortex, and striatum/thalamus ($P < 0.01$). At 24 hours, the ratios were significantly higher in hippocampus and cortex while at 3 and 7 days after HI permeability ratios were not different from controls. No

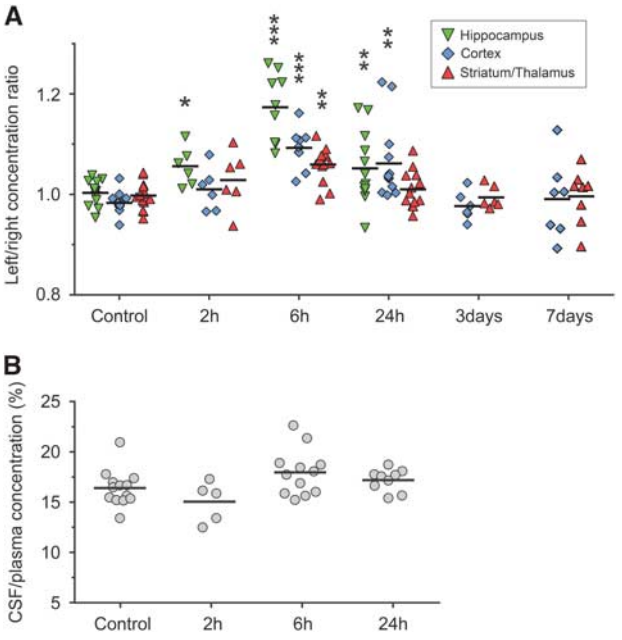

Figure 1. Blood–brain and blood–cerebrospinal fluid (CSF) barrier permeability after neonatal hypoxia-ischemia (HI). (**A**) Sucrose concentration ratios between the left (ligated) and right hemisphere in animals at different times after HI. Thus, ratios over 1 indicate an increase in blood–brain barrier permeability in the injured hemisphere. At 2 hours (2 hours), only hippocampal ratios were significantly higher than control values. The highest ratios were present at 6 hours after HI and these were significantly higher than control ratios in hippocampus, cortex, and in thalamus/striatum. Ratios were lower at 24 hours than at 6 hours but still significantly different in hippocampus and cortex from control values. At all other times and regions no statistical difference was detected between ratios. (**B**) Sucrose CSF/plasma concentration ratios in P9 control animals and at 2 to 24 hours after HI with no significant differences detected between HI and control animals. Data are mean ± s.e.m., $n = 6$ to 14/group; $^{*}P < 0.05$, $^{**}P < 0.01$, $^{***}P < 0.001$ compared with controls (ANOVA followed by LSD).

statistically significant differences were found in inulin brain/plasma ratios between the left and right hemisphere in any brain regions with a range of 1.09% to 1.43% in the average ratios across all brain regions and time points. Ratios in cerebellum and brainstem were almost identical between HI animals and naïve controls at all measured time points after HI (data not shown). There was no significant effect on CSF/plasma concentrations ratios after HI (Figure 1B).

Immunohistochemistry

MAP-2 and Albumin. We used MAP-2 to visualize infarct area and albumin to visualize regions of brain with compromised BBB at 2, 6, and 24 hours after HI. In aged-matched naïve animals, MAP-2 was associated with gray matter and albumin was only localized to cerebral blood vessels. At 2 hours after HI, the infarct was localized to the left hippocampus (ligation side) with occasional animals with infarcts in the thalamic regions close to the ventricle (Figure 2A). At 6 and 24 hours, a cortical infarct was often also observed. No infarct was visible in the right side of the brain in HI animals with no visible difference to the naïve control brain. Albumin was sometimes visible in the parenchyma of hippocampus at 2 hours after HI (4/5 animals) but none in other regions of the brain. At 6 and 24 hours, all animals showed parenchymal staining of albumin in hippocampus and also some in thalamic and cortical regions. Albumin staining was associated with infarct

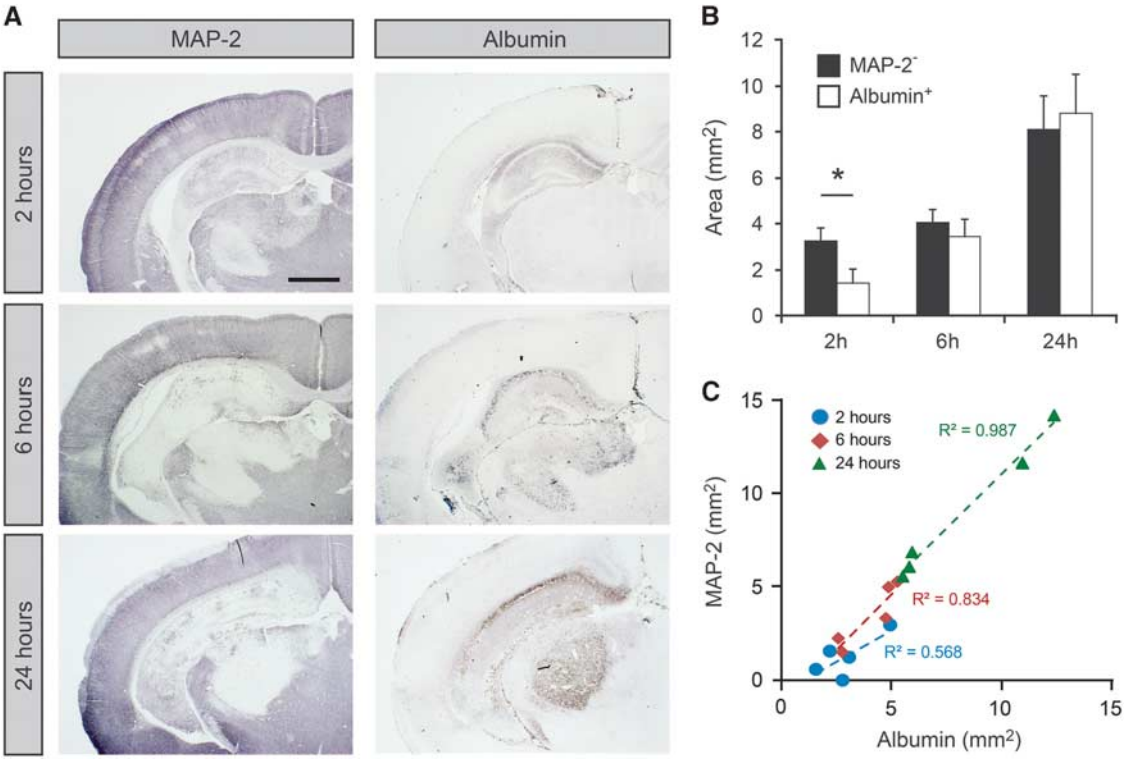

Figure 2. Infarct area and albumin extravasation after neonatal hypoxia-ischemia (HI). (**A**) Illustrations of MAP-2 and albumin immunoreactivity in tissue sections after HI. MAP-2 was used to delineate the infarct area and albumin was used to detect areas with compromised blood–brain barrier function to larger proteins. At 2 hours after HI, MAP-2 immunoreactivity was reduced in hippocampus in all animals and also in thalamus in some animals. With time MAP-2 staining was also lost in cortex (6 and 24 hours). Albumin was detected in hippocampus in some animals at 2 hours (4/5 animals). At 6 and 24 hours albumin was detected in hippocampus in all animals and sometimes also in thalamus and cortex. The albumin-positive area was always contained within the MAP-2-negative area and at 24 hours these two areas were almost identical in all animals. Scale bar is 1 mm. (**B**) Measurements of MAP-2-negative and albumin-positive areas of the brain sections. Measurements were made in two hippocampal sections from each animal and averaged. Both areas increased with time after HI. Data are mean ± s.e.m., $n = 5$/group; $^*P < 0.05$ (*t*-test). (**C**) Correlation of MAP-2-negative and Albumin-positive area across all animals and time points. There was a linear correlation of these two areas with almost identical slopes at 6 and 24 hours after HI.

area at all times after HI. Measurements of infarct area (MAP-2$^-$) and areas with protein leakage (albumin$^+$) were made from photomicrographs of pairs of stained sections (Figures 2B and 2C). This showed that at 2 hours about 40% of infarct area was also albumin$^+$ ($P < 0.05$), at 6 hours around 80% was albumin$^+$ and at 24 hours 108% was albumin$^+$ (Figure 2B). Data from individual animals showed that a linear correlation consisted between the two areas at 6 and 24 hours with almost identical slopes of regression lines ($r^2 = 0.83$ and 0.99, respectively).

Tight-junctional proteins. We performed immunoreactivity analysis for three key tight-junction associated proteins (claudin-5/occludin/ZO-1) in the brain to examine molecular damage to BBB after HI. In all areas of the brain, these proteins were associated with barrier-forming cells (cerebral blood vessels and choroidal epithelial cells) and none were apparent in brain parenchyma. This was similar in animals after HI and endothelial cells in infarct area were positive for all these proteins, see Figure 3A. Occludin and ZO-1 were also detected in the apical side of choroidal epithelial cells where the tight junctions are present (Figure 3B). This staining pattern was detected in all choroid plexuses at 2 to 24 hours after HI and there was no obvious difference in staining between injured and noninjured hemisphere as well as naïve control brains.

Staining pattern of claudin-5 was further analyzed at 6 hours after HI (the time point when the largest sucrose permeability increase was measured, see Figure 1), by confocal microscopy. Albumin was used to visualize areas with barrier dysfunction. In areas that showed no sign of albumin extravasation, claudin-5 showed a distinct pattern of expression on blood vessels with typical bands across and along cerebral vessels (see Figures 4A and 4C). In areas with albumin extravasation some vessels showed loss of this distinct expression pattern with more granular or diffuse immunoreactivity in blood vessels (Figures 4A and 4C).

Caspase-3 Activity, qPCR, and Western Blotting

Samples of hippocampus, cortex, and choroid plexuses were collected from the left and right hemispheres at 6 hours after HI, the time point with the highest BBB sucrose permeability after HI. Caspase-3 assays were initially performed on brain samples to confirm HI-related injury in tissues.

Caspase-3 activity assay. Caspase-3 activity was measured in all hippocampal and cortical samples ($n = 8$, respectively) that were further used for qPCR and western blotting. This showed that in the hippocampus no activity was found in the right hemisphere in any sample whereas in left hemisphere the average activity was 67.1 ± 10.5 pmol AMC/min × mg protein. In cortical samples from the right hemisphere the average activity was 5.2 ± 3.2 (activity detected in three samples) and 27.8 ± 5.4 pmol AMC/min × mg protein in the left cortex. Thus, the brain tissue samples used

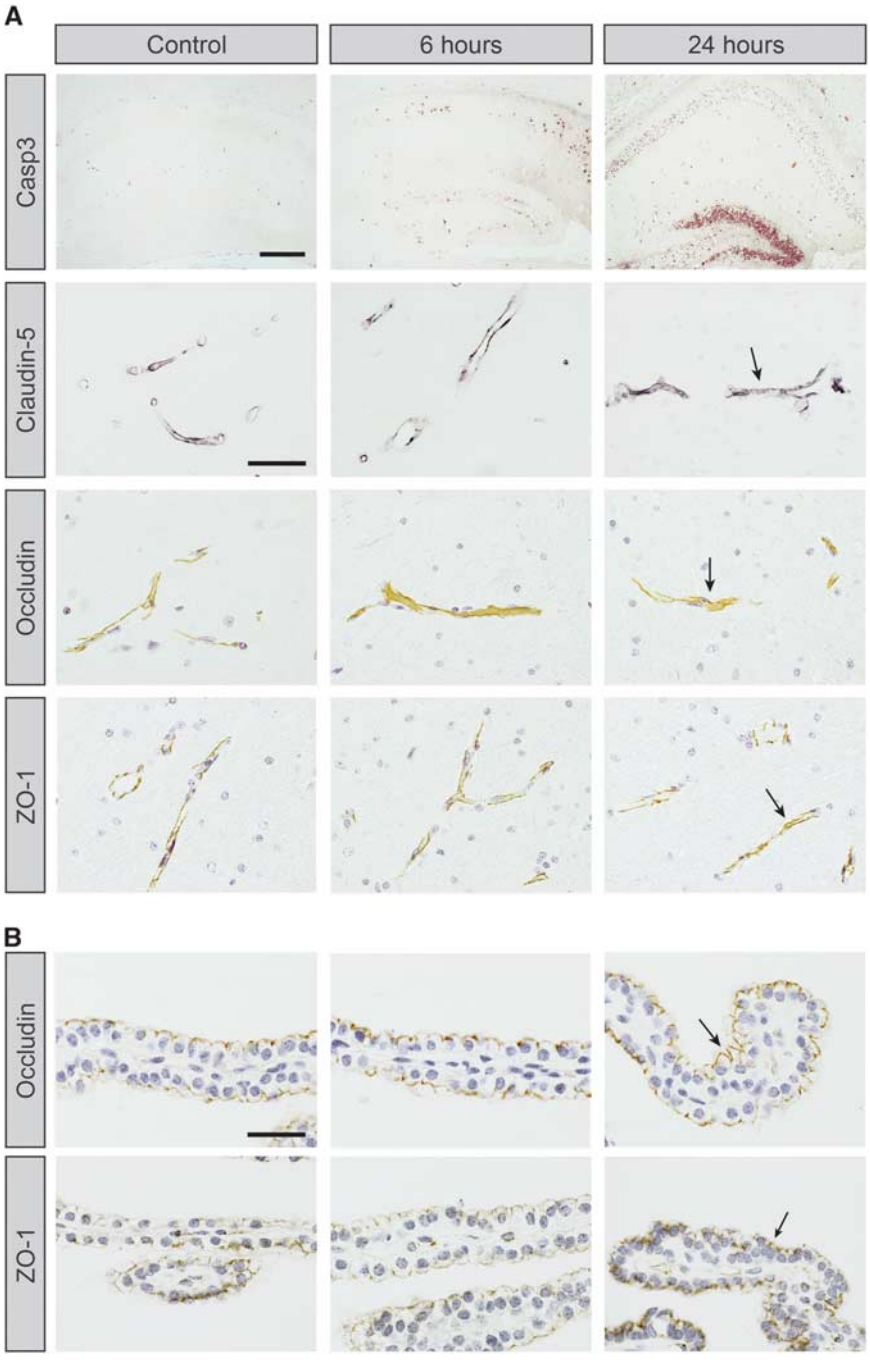

Figure 3. Immunoreactivity of caspase-3 and tight-junctional (tj) proteins on coronal sections of hippocampus and choroid plexus at 6 and 24 hours after neonatal hypoxia-ischemia (HI). (**A**) Number of caspase-3-positive cells is much greater at 6 and 24 hours after HI than in controls and is most abundant in the CA1 granular layer as well as the dentate gyrus. Note also that tissue degradation is visible in granular layer and distortion of hippocampus (possibly due to brain edema) could be seen in some animals at 24 hours. Despite damage to the hippocampus at 6 and 24 hours after HI, blood vessels were positive for tj-associated proteins (arrows). No immunoreactivity was detected in brain parenchyma for any of the tj proteins. Sections for caspase-3, occludin, and ZO-1 have been counterstained with hematoxylin. Scale bar is 200 μm (Casp3) and 40 μm (tj proteins). (**B**) Photomicrographs from telencephalic choroid plexuses. In sections from controls as well as animals at 6 and 24 hours the apical side of epithelial cells, where the tj proteins are present, is positive for occludin and ZO-1 (arrows). Sections counterstained with hematoxylin. Scale bar is 30 μm.

consistently showed injury-related caspase-3 activation in the left hemisphere.

Western blotting. Western blotting was performed on hippocampal and cortical samples from 6 hours after HI to detect levels of tight-junctional proteins. Protein levels in left hemisphere were normalized to right hemisphere in each animal and results presented in Figure 5A. Claudin-5 levels were not significantly changed whereas occludin levels were consistently lower in all hippocampal and cortical left side samples with a -2.28 ± 0.28

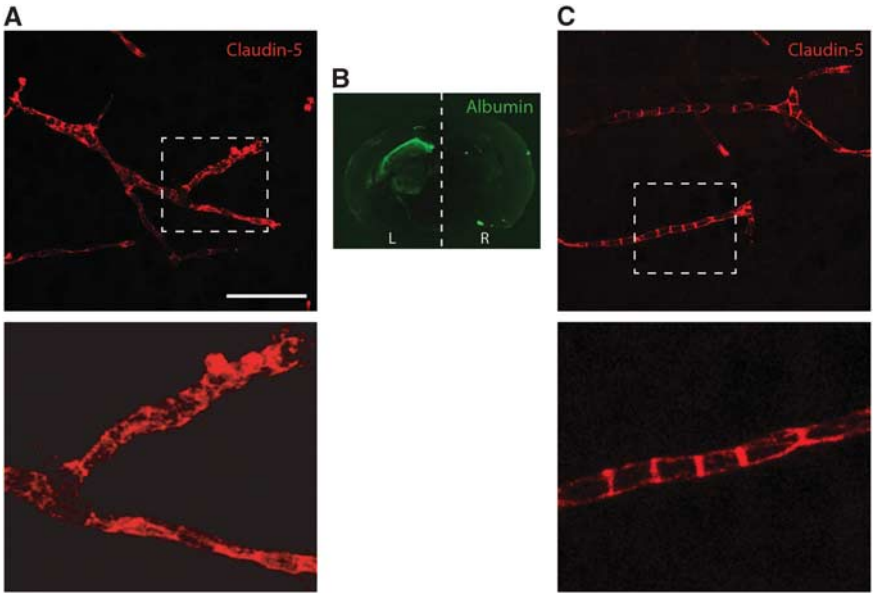

Figure 4. Immunoreactivity of claudin-5 on frozen sections from brain at 6 hours after hypoxia-ischemia in neonatal mice. 2D projections of Z-stacks obtained by confocal microscopy. (**A**) In areas with albumin extravasation within the brain the claudin-5 pattern of expression was granulated or diffuse throughout the blood vessels in some capillaries. Enlarged area is shown underneath. (**B**) Areas of compromised blood–brain barrier were visualized with albumin immunoreactivity. (**C**) In the right side of the brain the pattern of expression is similar to control animals with characteristic banded staining of blood vessels. Enlarged area is shown underneath. L, left (ligated) hemisphere; R, right hemisphere. Scale bar represents 50 μm in (**A** and **C**) and 15 μm for enlarged images.

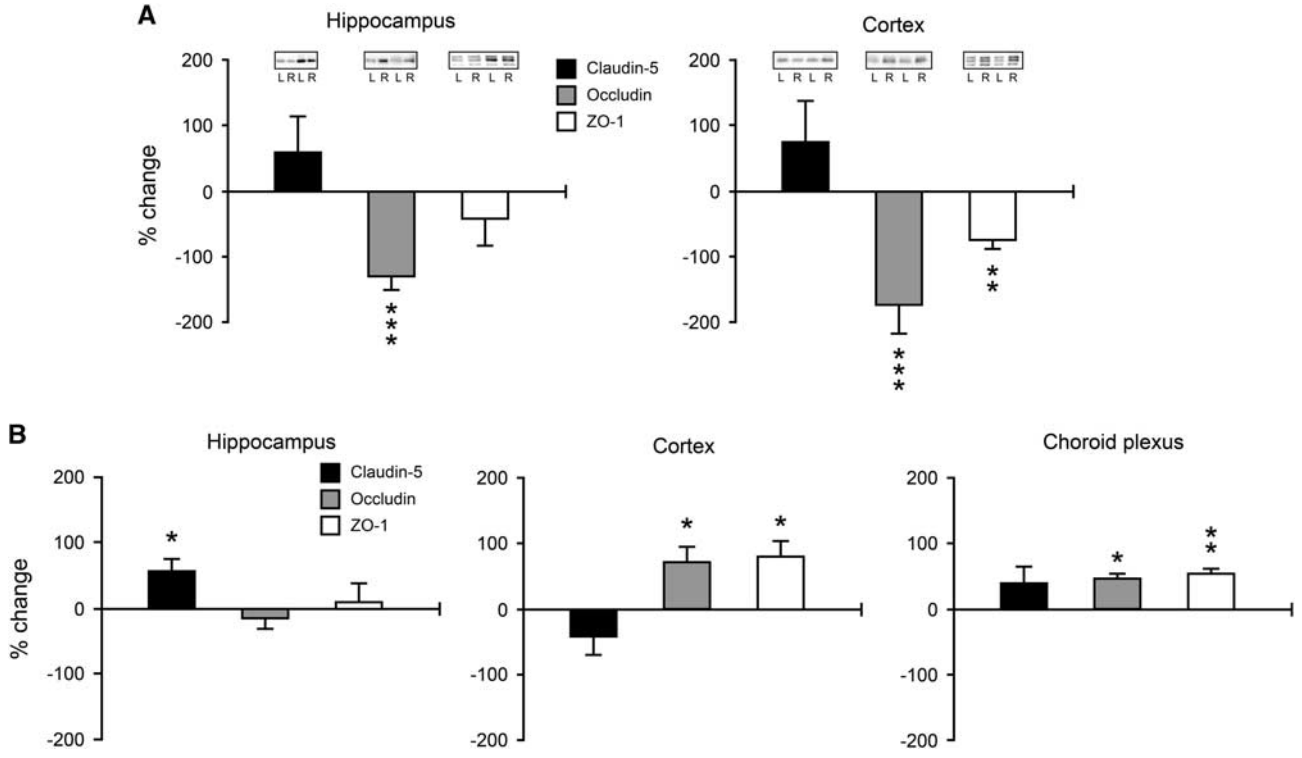

Figure 5. Protein and gene expression of tight-junctional proteins at 6 hours after neonatal hypoxia-ischemia (HI). (**A**) Semi-quantitative western blot analysis of claudin-5 (black bars), occludin (gray bars), and ZO-1 (white bars) protein in tissue samples from hippocampus and cortex at 6 hours after HI. All results presented as percent change between left (ligated) and right hemispheres. Occludin protein levels were significantly lower in left hippocampus and cortex, ZO-1 protein levels significantly lower in left cortex. Data are mean ± s.e.m., $n = 7$/group. (**B**) Gene expression of claudin-5, occludin, and ZO-1 in hippocampus and cortex as well as claudin-1, occludin, and ZO-1 in telencephalic choroid plexuses. All results presented as percent change between left (injured) and right hemisphere samples. There was a significantly higher gene expression of claudin-5 in left hippocampus, occludin and ZO-1 in left cortex, occludin and ZO-1 in left choroid plexus. Data are mean ± s.e.m., $n = 7$ to 8/group; $^{*}P < 0.05$, $^{**}P < 0.01$, $^{***}P < 0.001$ left compared with right hemisphere (*t*-test). L, left (ligated) hemisphere; R, right hemisphere.

and −2.73 ± 0.66 fold change, respectively, over right hemisphere samples ($P < 0.001$ for both groups). In addition, ZO-1 levels in left cortical samples were significantly lower over right hemisphere (−1.76 ± 0.20 fold change; $P < 0.01$).

Quantitative reverse-transcription PCR. Quantitative PCR was performed on hippocampal, cortical, and choroid plexus samples from 6 hours after HI (Figure 5B). Expression levels in left hemisphere samples were normalized to right hemisphere samples. There was an upregulation of many of the tight junction-associated mRNAs in the left hemisphere in tissues: significant upregulation was found in claudin-5 mRNA in hippocampus (1.59 ± 0.21 fold change; $P < 0.05$), in occludin and ZO-1 mRNA in cortex (1.69 ± 0.27 and 1.79 ± 0.29 fold higher, respectively; $P < 0.05$) and likewise in occludin and ZO-1 mRNA in choroid plexus (1.39 ± 0.11 and 1.44 ± 0.09 fold higher, respectively; $P < 0.05$ and $P < 0.01$, respectively).

Regional Cerebral Blood Flow

Cerebral blood flow was measured both during and after HI and results from autoradiographic measurements are presented in Figure 6 and complete results summarized in Figure 7. The rCBF based on calculations from autoradiograms in P9/P10 control brains amounted to between 33 and 58 mL/min × 100 g in the different brain regions with lowest values in white matter and highest in the thalamus. Blood flow at 30 minutes after induction of HI was much lower in left (ligated) hemisphere compared with controls with lowest value in the hippocampus (0.7 ± 0.5 mL/min × 100 g; $P < 0.001$ to controls) and highest in the medial parts of the cortex (28.5 ± 11.5 mL/min × 100 g; $P = 0.32$) whereas in the right (nonligated) hemisphere the blood flow was higher than in controls in all regions of the brain with the highest blood flow observed in the thalamus (153 mL/min × 100 g; $P = 0.03$), see Figure 6. The rCBF was lower at 50 minutes of HI in the left hemisphere compared with controls in all regions (lowest value in the hippocampus: 7.9 ± 3.4 mL/min × 100 g; $P < 0.001$) except the medial parts of the cortex (66.6 ± 26.0 mL/min × 100 g; $P = 0.084$) whereas in the right (nonligated) hemisphere the blood flow was higher than in controls in all regions of the brain with the highest rCBF in the thalamus (222.7 ± 86.7 mL/min × 100 g; $P < 0.001$). The rCBF in all brain regions was somewhat lower than in controls at 2 hours (significantly different to controls in left-white matter, -striatum, -hippocampus and right white matter) and in most brain regions at 6 hours (but none significantly different) after HI. In addition, rCBF in the more anterior or posterior parts of the medial/lateral cortex and white matter was calculated and we found very small differences in rostral vs. caudal sections in these brain regions (Figure 7A). In general, the cerebral blood in whole hemispheres measured by LSC agreed well with the average rCBF measured with autoradiography during control and HI as well as during postHI recovery (Figure 7B). Furthermore, ligation without hypoxic exposure did not alter CBF (Figure 7B).

DISCUSSION

We have studied CBF, permeability at brain barriers, and changes to tight-junctional proteins after an HI episode in neonatal mice to further our understanding of the underlying mechanisms leading to perinatal brain damage. This showed that there was a rapid but transient opening of the BBB which was associated with decreases in levels of several barrier proteins in brain as well as a change in the pattern of expression on cerebral vessels. However, there was an increase in mRNA levels of genes coding for tight-junctional proteins indicating that, in parallel, compensatory mechanisms are induced to restore normal BBB function. Regional cerebral blood flow experiments were conducted for the first time in awake nonanesthetized neonatal mice after HI showing that overall

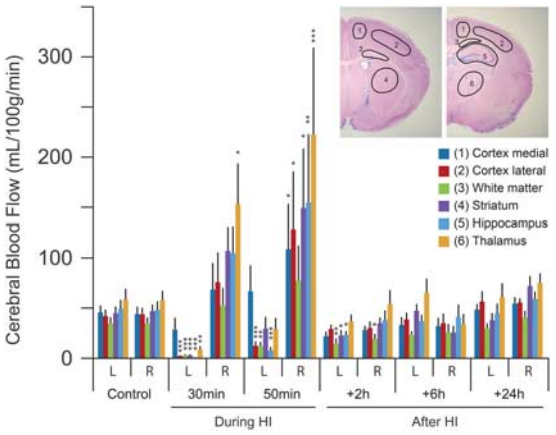

Figure 6. Regional cerebral blood flow during and after neonatal hypoxia-ischemia (HI) from autoradiograms. Brain regions for blood flow measurements are outlined to the top right. This shows a reduction in all brain regions of left (ligated) hemisphere, except the medial parts of the cortex, compared with controls whereas in the contralateral hemisphere blood flow was higher than controls during HI. Blood flow after HI was somewhat lower in some brain regions at 2 hours after HI but restored to near normal at 6 and 24 hours after HI in all brain regions. For examples of autoradiograms see Figure 7. Data are mean ± s.e.m., $n = 5$ to 8/group; $^*P < 0.05$, $^{**}P < 0.01$, $^{***}P < 0.001$ compared with controls (ANOVA followed by LSD). L, left (ligated) hemisphere; R, right hemisphere.

changes in blood flow were mostly similar to previous measurements in the neonatal rat although some regional differences were observed.

Changes to Brain Barrier Permeability after Hypoxia-Ischemia

There is today convincing evidence that many of these barrier mechanisms are already present in the developing animal at both the blood–brain and blood–CSF barriers.[16–20] This is probably important for the protection of the embryo/fetus against neurotoxic compounds during pregnancy as well as providing the growing brain with the necessary supply of nutrients. From this standpoint, dysfunctional barrier mechanisms at critical developmental stages of the brain could have long-term adverse outcomes on brain function. Dysfunction to brain barrier mechanisms is well established after adult hypoxia/stroke, however, we know less how the neonate responds to a hypoxic and ischemic insult. Changes to normal barrier function have been implicated in a number of experimental animal studies,[3] as well as in human babies exhibiting HIE,[21] although piglets have shown resistance to BBB dysfunction after hypoxia,[22] and mice unaltered BBB permeability in a newborn stroke model.[23] Muramatsu *et al*[24] found a successive decrease in BBB opening when insult was performed in P7, P14 or P21 animals. In P7 rats, which are probably the most equivalent developmental age to the P9 mice used in our study, extravasation of IgG was seen as early as 3 hours after HI corresponding to our early opening of the BBB after HI.

We have quantitatively measured sucrose accumulation as well as examined albumin extravasation in the brain to investigate BBB permeability after HI. In general, our results from these two ways of assessing BBB integrity were in agreement. Both methods showed an early opening of the BBB already at 2 hours after HI in the hippocampus (see Figures 1 and 2). At 6 hours, all areas investigated showed elevated sucrose permeability but the largest increase was in the hippocampus. At 24 hours, the elevated sucrose BBB permeability had somewhat resolved and at 3/7 days after HI BBB sucrose permeability was not significantly different from control animals. Thus, our results indicate a rapid opening of the barrier but also restoration of barrier function in the days after

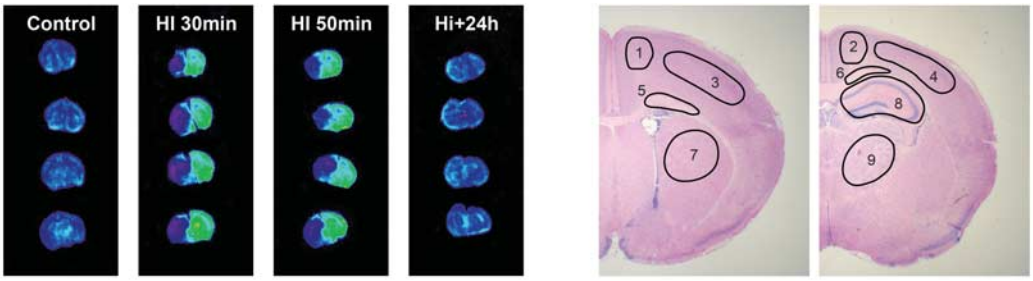

A

	Control (8)		HI 30min (5)		HI 50min (5)		+2h (5)		+6h (5)		+24h (5)	
	L	R	L	R	L	R	L	R	L	R	L	R
Cortex medial ante. (1)	46.5±6.7	46.3±7.4	29.4±12.9	68.3±25.8	70.8±26.2	116.4±47.5	23.3±4.3	31.7±6	37.4±7.9	35.6±7.5	54±8.5	66.2±11.1
Cortex medial post. (2)	44.9±7.5	41.9±7.4	27.7±11.4	68.8±27.8	62.5±26.2	101.3±42.2	20.4±6.6	24.3±5.4	28.7±8.2	28.6±9.3	43.1±5.5	42.8±4.2
Cortex lateral ante. (3)	45.0±7.1	45.9±6.9	1.5±0.4	76.6±29.4	12.7±5.3	139.3±60.8	32.7±5.1	34.5±6.1	42.8±7.1	39.9±10.9	64±12.6	64.9±7.0
Cortex lateral post. (4)	39.1±6.3	41.6±6.9	2.8±1.2	75.3±30.5	12.1±4.5	117.4±54.5	25.8±4.0	25.6±7.9	34.6±7	30.0±8.3	49±9.6	46.4±4.2
White matter ante. (5)	33.7±6.1	33.5±6.1	2.3±1.5	50.3±16.6	13.7±5.5	70.8±30.3	14±6.0	19.1±5.7	26.1±4.5	25.6±7.9	30.9±5.2	45.7±8.8
White matter post. (6)	35.9±6.6	35.6±6.5	3.1±1.3	55.0±18.8	10.5±4.5	83.3±40.8	14.7±5.0	19.3±5.8	20.4±3.5	25.2±9.5	28.6±6.2	35.9±5.7
Striatum (7)	44.9±6.6	46.8±6.7	3.0±0.8	107.1±23.7	29.5±11.6	149.4±59.2	22.6±5.6	35±5.6	47.3±7.0	25.6±6.6	37.8±7.2	72±10.0
Hippocampus (8)	49.5±8.7	48.4±8.4	0.7±0.5	104.7±26.7	7.9±3.4	154.8±68.3	23.4±4.0	38.1±9.6	37.1±6.2	41.0±12.6	44.8±9.6	59.1±7.4
Thalamus (9)	58.8±10.4	57.8±9.5	8.9±3.1	153.1±40.6	29.2±11	222.7±86.7	36.5±7.1	54.1±14.1	65.4±13.9	33.9±10.2	61±13.8	75.3±9.3

B

Control (8)	Ligation (15)		HI 30min (5)		HI 50min (10)		+2h (5)		+6h (5)		+24h (5)	
	L	R	L	R	L	R	L	R	L	R	L	R
54.6±5.0	55.6±3.6	57.3±3.6	21.8±4.1$^{\#}$	117.2±16.1$^{\#}$	38.2±5.6$^{¤}$	80.4±10.8	40.4±4.5	59.9±15.9	63.5±12.6	73.4±9.5	47.5±6.7	52.5±6.7

Figure 7. Regional cerebral blood flow (rCBF) measurements (mL/100 g per minute) by the iodoantipyrine method during and after HI using both calculations from autoradiograms in nine brain regions (**A**) and liquid scintillation counting (LSC) of whole brain hemispheres (**B**). The results of the two methodological approaches for measurement of CBF after iodoantipyrine injections were comparable. In addition to results in this figure, the anterior and posterior parts of the medial/lateral and white matter are presented. Small differences were found be tween the anterior/posterior parts in these brain regions although rCBF was almost always somewhat lower in the more posterior parts of medial and lateral cortex. Note also that in animals with left carotid artery ligation only (without HI) CBF at 1 hour after the ligation was near to identical with control animals (see **B**). Examples of autoradiograms (four levels/animal) are shown above the table where gray scale images have been converted to rainbow color spectrums to more clearly visualize the changes in rCBF. The nine regions for rCBF measurements are shown in top right. Data are mean ± s.e.m., number of animal for each group in brackets. Outcome of statistical analysis only presented for data in (**B**) (see Figure 6 for rCBF). $^{¤}P < 0.01$, $^{\#}P < 0.001$ (ANOVA followed by LSD). L, left (ligated) hemisphere; R, right hemisphere.

the insult. It should also be mentioned that albumin could be detected in brain sections still at 3 days after the insult (not illustrated) but considering that sucrose permeability is restored at this point this may be due to slow clearance of albumin in tissue after the insult and not due to a leaky BBB. However, since these molecules do have different molecular properties we cannot rule out that albumin may still cross the BBB at a higher rate than normal for longer times than sucrose. Since albumin extravasation shows the accumulation in brain until the protein is fixed it is very difficult to exactly know to which extent and when the extravasation occurred. Overall, this study clearly shows BBB leakage of both small and large molecules after neonatal HI. We could not detect any changes of sucrose permeability at the blood–CSF barrier after HI. This result is in agreement with previous studies by us where we found that the choroid plexus is not damaged after neonatal HI in mice.[25] However, since similar studies in the rat have shown considerable damage to the choroid plexus,[26] the outcome on the blood–CSF barrier may be species specific in this model. As discussed further below, we found a potent blood circulation in brain tissues up until at least 24 hours after HI (see Figures 6 and 7) as well as little differences in vascular space of the brain (determined by near-end experiment brain inulin ratios) strongly indicating that the increases in sucrose accumulation in brain observed after HI are due to alterations in BBB permeability and not other vascular factors.

Changes in Permeability in Relation to Neuropathology

There was a robust correlation between the infarct area and the area of albumin extravasation after HI (Figure 2). This shows a close relationship between BBB dysfunction and neuropathology after neonatal HI. Since one of the fundamental roles of the BBB is to protect the brain from blood-borne compounds this close relationship makes it is likely that the opening of the BBB, at least partially, contributes to the neuropathology. One could speculate that the reason for the close relationship between BBB dysfunction and neuropathology is that they do influence each other in a negative way whereby opening of the BBB leads to damage and heightened inflammation in the brain, via influx of blood solutes such as inflammatory mediators, and that this in turn leads to an increase in BBB opening and/or vice versa. The primary cause of the injury is the acute insufficient energy supply resulting from the very low blood flow occurring during the hypoxic phase in the left brain hemisphere (see Figures 6 and 7). As seen in Figure 6, restoration of blood flow does occur fairly rapidly after the hypoxic phase but within hours after the insult a cascade of inflammatory

mediators inside the brain are released;[27] although data on the inflammatory response in periphery are scarce global sheep models of hypoxia show that IL-1β levels are rapidly increased after insult,[28] and HIE in humans newborns is also associated with higher cytokine blood levels.[29,30] While BBB is compromised there is higher potential for signaling systems, such as inflammatory mediators, in brain and periphery to influence each other in a detrimental way. Since our study shows such a close relationship between BBB opening and infarct area, the BBB appears as an attractive therapeutic target to limit HI-induced brain damage. Previous studies in sheep to restore BBB function after perinatal brain damage have had promising results[31] along with recent studies in rats.[32]

Changes in Barrier Proteins after Neonatal Hypoxia-Ischemia

To understand the underlying mechanisms for BBB opening, we have studied the gene and protein expression of three key tight-junction related proteins (see more below). Quantification of tight-junctional proteins was possible in brain tissue, but not in choroid plexus due to the small sample size of tissue. Tight-junction expression was investigated at 6 hours after HI since this was the time point when we could detect the largest increase in BBB permeability (see Figure 1). We found changes in both the level and in the cellular distribution of tight-junction proteins after neonatal HI in the brain. In both hippocampus and cortex, the protein content of occludin more than halved in the left (ligated) compared with the nonligated side as well as a significant reduction of ZO-1 protein in the cortex (Figure 5A). In parallel, we examined the cellular location of these proteins within the brains after HI. In all brains studied, these three proteins only localized to the barrier forming cells. Examination of paraffin sections revealed no change in tight-junction protein staining after HI. Since claudin-5 has been shown to be a key protein at the BBB[11] we further analyzed this with confocal microscopy. This showed a distinct pattern of staining, see Figure 4, with banded staining of cerebral blood vessels and that a small number of vessels, within the area of left hemisphere that also showed a loss of BBB integrity to albumin, the banded appearance of caudin-5 immunoreactivity was lost and protein localized more uniform within the vessels. This shows that BBB opening after HI is associated with distinct changes in tight-junctional protein expression. However, it is difficult to exactly understand how these molecular changes may compromise BBB function since much it is still unclear of the molecular architecture, interactions, and regulation of tight junctions. That the loss of claudin-5 can directly affect BBB function is apparent from a study by Nitta *et al*.[11] The role of occludin at the tight junction remains obscure and although animals lacking occludin have been shown to be able to assemble functional tight junctions,[33] subsequent studies have found that phosphorylation state of certain Ser/Thr residues is linked to either disassembly or assembly of tight junction.[34] The ZO proteins appear to be critical for normal tight-junctional scaffolding but loss of protein in mature tight junctions is believed to be less critical for tight-junctional properties.[35]

One noteworthy finding of this study was that in parallel with the loss of tight-junctional proteins in the brain, the mRNA of several of these proteins was increased. This suggests that it is unlikely to be transcriptional regulation that is responsible for the loss of tight-junction proteins or barrier function. On the contrary it appears that after the insult, mechanisms are induced promoting tight-junctional formation. Since barrier opening is resolved in the days after the insult these mechanisms may be one important part of the neuroprotective mechanisms after the insult. An interesting aspect of this is that although the choroid plexus seems not to be damaged by the insult, as we have shown in previous studies,[25] and that we cannot detect a change in BCB function, there is still an induction of barrier protein mRNA at the BCB. It therefore appears possible that some kind of soluble factor is responsible for this induction of tight-junctional mRNA at both the BBB and the BCB. It was recently proposed that astrocytes secrete sonic hedgehog, which can promote tight-junction proteins at the BBB.[36]

Regional Cerebral Blood Flow

We measured regional and whole brain CBF before, during, and after HI (Figures 6 and 7). The most profound decrease of CBF in the left hemisphere occurred in the middle of the hypoxic exposure with severe reductions in almost all measured brain regions (1.5% to 15% of control values) except the medial parts of the cortex (62% of controls). In contrast, a substantial increase in rCBF (50% to 165% increase) was found in the right (nonligated) side. A similar pattern was seen at the end of the hypoxia although the reductions in the left hemisphere (16% to 66% of control values) were not as severe as found in the middle of hypoxia, whereas a further increase in rCBF was detected in the right hemisphere (111% to 285% increase). After hypoxia, the rCBF was somewhat lower than in control brains in both hemispheres and slowly returned to the normal range 2 to 6 hours after the hypoxia with little differences between the left and right hemispheres. The similar rCBF between left/right hemispheres and the maintenance of rCBF after HI indicates that blood flow is not an influencing factor for the assessments of barrier permeability. The pattern of reduced rCBF during HI correlates very well with the pattern of injury in this (MAP-2 loss) and previous studies in mice[9,37] as well as the regional opening of the BBB. The pattern of changes in rCBF during HI is quite comparable to previous studies using autoradiography in rats[8] although with some distinct differences. Comparisons of exact values between studies might be misleading since it will depend on the areas selected for rCBF. However, during the hypoxia in the rat after unilateral ligation, the most severe reductions in rCBF occurred in the parietal cerebral cortex whereas in mice the decrease in rCBF was most pronounced in the hippocampus.[7] Furthermore, the increase in rCBF in the nonligated contralateral hemisphere was more pronounced in mice than in rats (c.f. [8]). Furthermore, during postHI reperfusion there is a rapid recovery (and sometimes an overshoot) of CBF in rats[6] up to 24 hours followed by a delayed decrease in CBF at 48 to 72 hours particularly in injured areas.[5,6] In mice, there was a more gradual return of rCBF to normal levels over 2 to 6 hours in both hemispheres. However, in agreement with CBF measurements in rats there was a rapid return of blood flow in the normal range suggesting that no-reflow phenomena is not a major contributor in the secondary injury process in this model. The CBF in the cerebral cortex has also been measured with the laser doppler flow (LDF) and laser speckle technology in immature mouse pups subjected to HI.[38,39] According to those measurements, CBF in the cortex decreases markedly in both the ipsi- (ligated) and contralateral hemispheres during the hypoxic exposure and recovery of CBF appears incomplete at 150 minutes, 9 hours, and 24 hours.[38,39] The explanation for this discrepancy compared with our results is unclear but could relate to our measurements having been performed in awake animals rapidly decapitated at different time points whereas LSD and laser speckle measurements were performed on the surface of the brain after surgical preparation and under anesthesia. It is interesting to note that CBF is not affected by ligation itself in this strain of mice (C57Bl/6), whereas in at least some CD-1 mouse strains unilateral carotid ligation decreases CBF to the extent that brain injury is induced.[40]

CONCLUSIONS

The main finding of this study is that there is rapid but transient opening of the BBB to small and larger compounds after HI in neonatal mice. The opening of BBB is associated with several

changes of tight-junctional proteins in the brain. The regions with brain damage correlate well with the regions of barrier opening as well as the regions with reduced rCBF during the hypoxia. However, it should also be noted that CBF and BBB function in newborns does show resilience to HI in that blood flow is maintained in infarcted areas at least up to 24 hours and that compensating mechanisms to tighten the barrier also seem to be activated after the insult. The timing of the opening of the barrier is important in relation to potential therapies since this provides a window of opportunity when compounds can more readily access the injured regions of the brain to ameliorate the damage. At the same time, the opening of the BBB is likely in itself to be partially responsible for the damage to the brain tissue so understanding the mechanism of barrier opening provides therapeutic targets.

DISCLOSURE/CONFLICT OF INTEREST

The authors declare no conflict of interest.

REFERENCES

1 Edwards AD, Brocklehurst P, Gunn AJ, Halliday H, Juszczak E, Levene M *et al.* Neurological outcomes at 18 months of age after moderate hypothermia for perinatal hypoxic ischaemic encephalopathy: synthesis and meta-analysis of trial data. *BMJ* 2010; **340**: c363.
2 Saunders NR, Ek CJ, Habgood MD, Dziegielewska KM. Barriers in the brain: a renaissance? *Trends Neurosci* 2008; **31**: 279–286.
3 Baburamani AA, Ek CJ, Walker DW, Castillo-Melendez M. Vulnerability of the developing brain to hypoxic-ischemic damage: contribution of the cerebral vasculature to injury and repair? *Front Physiol* 2012; **3**: 424.
4 Hawkins BT, Davis TP. The blood-brain barrier/neurovascular unit in health and disease. *Pharmacol Rev* 2005; **57**: 173–185.
5 Gilland E, Bona E, Hagberg H. Temporal changes of regional glucose use, blood flow, and microtubule-associated protein 2 immunostaining after hypoxia-ischemia in the immature rat brain. *J Cereb Blood Flow Metab* 1998; **18**: 222–228.
6 Mujsce DJ, Christensen MA, Vannucci RC. Cerebral blood flow and edema in perinatal hypoxic-ischemic brain damage. *Pediatr Res* 1990; **27**: 450–453.
7 Ringel M, Bryan RM, Vannucci RC. Regional cerebral blood flow during hypoxia-ischemia in the immature rat: comparison of iodoantipyrine and iodoamphetamine as radioactive tracers. *Brain Res Dev Brain Res* 1991; **59**: 231–235.
8 Vannucci RC, Lyons DT, Vasta F. Regional cerebral blood flow during hypoxia-ischemia in immature rats. *Stroke* 1988; **19**: 245–250.
9 Hedtjärn M, Leverin AL, Eriksson K, Blomgren K, Mallard C, Hagberg H. Interleukin-18 involvement in hypoxic-ischemic brain injury. *J Neurosci* 2002; **22**: 5910–5919.
10 Ek CJ, Habgood MD, Dziegielewska KM, Potter A, Saunders NR. Permeability and route of entry for lipid-insoluble molecules across brain barriers in developing Monodelphis domestica. *J Physiol* 2001; **536**: 841–853.
11 Nitta T, Hata M, Gotoh S, Seo Y, Sasaki H, Hashimoto N *et al.* Size-selective loosening of the blood-brain barrier in claudin-5-deficient mice. *J Cell Biol* 2003; **161**: 653–660.
12 Wang X, Karlsson JO, Zhu C, Bahr BA, Hagberg H, Blomgren K. Caspase-3 activation after neonatal rat cerebral hypoxia-ischemia. *Biol Neonate* 2001; **79**: 172–179.
13 Gilland E, Hagberg H. NMDA Receptor-dependent increase of cerebral glucose utilization after hypoxia-ischemia in the immature rat. *J Cereb Blood Flow Metab* 1996; **16**: 1005–1013.
14 Maeda K, Mies G, Olah L, Hossmann KA. Quantitative measurement of local cerebral blood flow in the anesthetized mouse using intraperitoneal [14C]iodoantipyrine injection and final arterial heart blood sampling. *J Cereb Blood Flow Metab* 2000; **20**: 10–14.
15 Sakurada O, Kennedy C, Jehle J, Brown JD, Carbin GL, Sokoloff L. Measurement of local cerebral blood flow with iodo [14C] antipyrine. *Am J Physiol* 1978; **234**: H59–H66.
16 Ek CJ, Dziegielewska KM, Stolp H, Saunders NR. Functional effectiveness of the blood-brain barrier to small water-soluble molecules in developing and adult opossum (Monodelphis domestica). *J Comp Neurol* 2006; **496**: 13–26.
17 Virgintino D, Errede M, Robertson D, Capobianco C, Girolamo F, Vimercati A *et al.* Immunolocalization of tight junction proteins in the adult and developing human brain. *Histochem Cell Biol* 2004; **122**: 51–59.
18 Kratzer I, Vasiljevic A, Rey C, Fevre-Montange M, Saunders N, Strazielle N *et al.* Complexity and developmental changes in the expression pattern of claudins at the blood–CSF barrier. *Histochem Cell Biol* 2012; **138**: 861–879.
19 Ballabh P, Hu F, Kumarasiri M, Braun A, Nedergaard M. Development of Tight Junction Molecules in Blood Vessels of Germinal Matrix, Cerebral Cortex, and White Matter. *Pediatr Res* 2005; **58**: 791–798.
20 Daneman R, Zhou L, Kebede AA, Barres BA. Pericytes are required for blood–brain barrier integrity during embryogenesis. *Nature* 2010; **468**: 562–566.
21 Kumar A, Mittal R, Khanna HD, Basu S. Free radical injury and blood-brain barrier permeability in hypoxic-ischemic encephalopathy. *Pediatrics* 2008; **122**: e722–e727.
22 Stonestreet BS, Burgess GH, Cserr HF. Blood-brain barrier integrity and brain water and electrolytes during hypoxia/hypercapnia and hypotension in newborn piglets. *Brain Res* 1992; **590**: 263–270.
23 Fernandez-Lopez D, Faustino J, Daneman R, Zhou L, Lee SY, Derugin N *et al.* Blood-brain barrier permeability is increased after acute adult stroke but not neonatal stroke in the rat. *J Neurosci* 2012; **32**: 9588–9600.
24 Muramatsu K, Fukuda A, Togari H, Wada Y, Nishino H. Vulnerability to cerebral hypoxic-ischemic insult in neonatal but not in adult rats is in parallel with disruption of the blood-brain barrier. *Stroke* 1997; **28**: 2281–2288.
25 D'Angelo B, Ek CJ, Sandberg M, Mallard C. Expression of the Nrf2-system at the blood-CSF barrier is modulated by neonatal inflammation and hypoxia-ischemia. *J Inherit Metab Dis* 2013; **36**: 479–490.
26 Rothstein RP, Levison SW. Damage to the choroid plexus, ependyma and subependyma as a consequence of perinatal hypoxia/ischemia. *Dev Neurosci* 2002; **24**: 426–436.
27 Hagberg H, Gressens P, Mallard C. Inflammation during fetal and neonatal life: implications for neurologic and neuropsychiatric disease in children and adults. *Ann Neurol* 2012; **71**: 444–457.
28 Prout AP, Frasch MG, Veldhuizen RA, Hammond R, Ross MG, Richardson BS. Systemic and cerebral inflammatory response to umbilical cord occlusions with worsening acidosis in the ovine fetus. *Am J Obstet Gynecol* 2010; **202**: e1–e9.
29 Shalak LF, Laptook AR, Jafri HS, Ramilo O, Perlman JM. Clinical chorioamnionitis, elevated cytokines, and brain injury in term infants. *Pediatrics* 2002; **110**: 673–680.
30 Silveira RC, Procianoy RS. Interleukin-6 and tumor necrosis factor-alpha levels in plasma and cerebrospinal fluid of term newborn infants with hypoxic-ischemic encephalopathy. *Pediatrics* 2003; **143**: 625–629.
31 Stonestreet BS, Petersson KH, Sadowska GB, Pettigrew KD, Patlak CS. Antenatal steroids decrease blood-brain barrier permeability in the ovine fetus. *Am J Physiol* 1999; **276**: R283–R289.
32 Hsu YC, Chang YC, Lin YC, Sze CI, Huang CC, Ho CJ. Cerebral microvascular damage occurs early after hypoxia-ischemia via nNOS activation in the neonatal brain. *J Cereb Blood Flow Metab* 2014; **34**: 668–676.
33 Saitou M, Fujimoto K, Doi Y, Itoh M, Fujimoto T, Furuse M *et al.* Occludin-deficient embryonic stem cells can differentiate into polarized epithelial cells bearing tight junctions. *J Cell Biol* 1998; **141**: 397–408.
34 Rao R. Occludin phosphorylation in regulation of epithelial tight junctions. *Ann NY Acad Sci* 2009; **1165**: 62–68.
35 Bauer H, Zweimueller-Mayer J, Steinbacher P, Lametschwandtner A, Bauer HC. The dual role of zonula occludens (ZO) proteins. *J Biomed Biotechnol* 20102010 40259.
36 Alvarez JI, Dodelet-Devillers A, Kebir H, Ifergan I, Fabre PJ, Terouz S *et al.* The hedgehog pathway promotes blood-brain barrier integrity and CNS immune quiescence. *Science* 2011; **334**: 1727–1731.
37 Hagberg H, Wilson MA, Matsushita H, Zhu C, Lange M, Gustavsson M *et al.* PARP-1 gene disruption in mice preferentially protects males from perinatal brain injury. *J Neurochem* 2004; **90**: 1068–1075.
38 Ohshima M, Tsuji M, Taguchi A, Kasahara Y, Ikeda T. Cerebral blood flow during reperfusion predicts later brain damage in a mouse and a rat model of neonatal hypoxic-ischemic encephalopathy. *Exp Neurol* 2012; **233**: 481–489.
39 Taniguchi H, Anacker C, Wang Q, Andreasson K. Protection by vascular prostaglandin E2 signaling in hypoxic-ischemic encephalopathy. *Exp Neurol* 2014; **255**: 30–37.
40 Comi AM, Weisz CJ, Highet BH, Johnston MV, Wilson MA. A new model of stroke and ischemic seizures in the immature mouse. *Pediatr Neurol* 2004; **31**: 254–257.

Supplementary Information accompanies the paper on the Journal of Cerebral Blood Flow & Metabolism website (http://www.nature.com/jcbfm)